Published OnlineFirst July 17, 2018; DOI: 10.1158/2326-6066.CIR-17-0712

Research Article

Cancer Immunology Research

Wnt3a/β-Catenin Signaling Conditions Differentiation of Partially Exhausted T-effector Cells in Human Cancers

Valeria Schinzari[1], Eleonora Timperi[1], Giulia Pecora[1], Francesco Palmucci[1], Daniela Gallerano[1], Alessio Grimaldi[1], Daniela Angela Covino[1], Nicola Guglielmo[2], Fabio Melandro[2], Emy Manzi[3], Andrea Sagnotta[3,4], Francesco Lancellotti[5], Luca Sacco[5], Piero Chirletti[5], Gian Luca Grazi[3], Massimo Rossi[2], and Vincenzo Barnaba[1,6,7]

Abstract

In this study, we investigated the role of the Wnt/β-catenin signaling pathway in antitumor immune responses. We report that the concentration of secreted Wnt3a was significantly higher in conditioned medium from tumor or nontumor tissues obtained from all hepatocellular carcinoma or colorectal cancer patients tested, than in serum of healthy donors or patients. In addition, both Wnt3a and β-catenin were overexpressed by tumor-infiltrating and nontumor-infiltrating $CD4^+$ or $CD8^+$ T cells. The majority of these T cells expressed a dysfunctional effector memory $Eomes^+T\text{-}bet^-$phenotype that we defined as partially exhausted, because they performed effector functions (in terms of interferon-γ and tumor necrosis factor-α production, as well as CD107a mobilization) despite their PD-1 expression. Wnt3a/β-catenin signaling in T naïve cells *in vitro* recapitulated the T-cell setting *in vivo*. Indeed, the differentiation of cultured T naïve cells was arrested, producing cells that resembled the $Eomes^{high}T\text{-}bet^{low}\beta\text{-}catenin^{high}$ T cells with moderate effector functions that infiltrated tumor and nontumor areas. Wnt3a blockade improved the capacity of T naïve cells to differentiate into effector cells *in vitro*. However, Wnt3a blockade did not affect the function and phenotype of differentiated, partially exhausted, tumor-infiltrating T cells *ex vivo*. Taken together, our data suggest that Wnt3a blockade halts the capacity of Wnt/β-catenin signaling to inhibit the differentiation of T naïve cells, but it does not restore the dysfunction of differentiated T cells, in the tumor setting. *Cancer Immunol Res; 6(8); 941–52. ©2018 AACR.*

Introduction

Wnt signaling depends on various ligand/receptor combinations between 19 Wnt proteins, 10 Frizzled receptors (FzdR), two coreceptors [such as low-density lipoprotein receptor-related protein 5 (LPR5 and LPR6)], or non-FzdRs. Wnt signaling induces intracellular signals involved in several processes, including embryonic development, carcinogenesis, stem cell maintenance, cell proliferation, survival, migration, differentiation, and T-cell development and differentiation (1–3). At least three Wnt signaling pathways from the ligand/receptor interactions listed above involve Wnt/β-catenin signaling (4). In the absence of a Wnt ligand, intracellular β-catenin is regulated by the "destruction complex." The destruction complex is composed of two scaffolding and tumor suppressor proteins, adenomatosis polyposis coli and axis inhibition protein (Axin1), and the serine/threonine kinases casein (CK1) and glycogen synthase kinase 3β (GSK3β). The destruction complex enables phosphorylation of β-catenin, which becomes accessible to ubiquitylination and proteasomal degradation (4, 5). In these conditions, β-catenin does not translocate into the nucleus and the T-cell factor/lymphocyte enhancer binding (Tcf/Lef) transcription factor silences Wnt target genes by interacting with a transcriptional repressor complex. If an FzdR and LPR5 or LPR6 coreceptors are engaged by a Wnt ligand, the downstream Wnt/β-catenin signaling cascade is triggered through the destruction complex CK1 and GSK3β proteins. LPR5 or LPR6 is phosphorylated, which allows Axin1 to dock. This, in turn, leads to inhibition of the phosphorylation and degradation of β-catenin. The β-catenin accumulation leads to its translocation into the nucleus, where the formation of complexes of β-catenin with Tcf/Lef family members (e.g., Lef1, Tcf1, Tcf3, and Tcf4) drives transcription of Wnt target genes. The Wnt/β-catenin signaling pathway is controlled by negative feedback mechanisms (6). Somatic mutations in genes encoding Wnt/β-catenin pathway components can induce aberrant Wnt signaling, which can lead to tumors such as colorectal cancer and hepatocellular carcinoma (HCC; refs. 4, 7), in which the accumulation of

[1]Dipartimento di Medicina Interna e Specialità Mediche, "Sapienza" Università di Roma, Policlinico Umberto I, Rome, Italy. [2]Dipartimento di Chirurgia Generale e Trapianti d'Organo, "Sapienza" Università di Roma, Policlinico Umberto I, Rome, Italy. [3]Chirurgia Epato-Bilio-Pancreatica, Istituto Nazionale dei Tumori "Regina Elena," Rome, Italy. [4]Dipartimento di Scienze Medico-Chirurgiche e Medicina Traslazionale, "Sapienza" Università di Roma, Azienda Ospedaliera Sant'Andrea, Rome, Italy. [5]Dipartimento di Scienze Chirurgiche, "Sapienza" Università di Roma, Policlinico Umberto I, Rome, Italy. [6]Pasteur-Fondazione Cenci Bolognetti, Rome, Italy. [7]Center for Life Nano Science, Istituto Italiano di Tecnologia, Rome, Italy.

Note: Supplementary data for this article are available at Cancer Immunology Research Online (http://cancerimmunolres.aacrjournals.org/).

V. Schinzari and E. Timperi contributed equally to this article.

Current address for E. Timperi: Institut Curie, PSL Research University, INSERM, Paris, France.

Corresponding Author: Vincenzo Barnaba, "Sapienza" Università di Roma, Viale del Policlinico 155, 00161 Rome, Italy. Phone: 390-649-1268; Fax: 390-649-383333; E-mail: vincenzo.barnaba@uniroma1.it

doi: 10.1158/2326-6066.CIR-17-0712

Published OnlineFirst July 17, 2018; DOI: 10.1158/2326-6066.CIR-17-0712

β-catenin or Wnt3a in cancer cells has been correlated with a poor prognosis (8, 9). In these conditions, the production of Wnt proteins is upregulated by cancer cells, thus establishing a vicious circle sustaining the Wnt/β-catenin signaling pathway (10).

Wnt/β-catenin signaling in mature T-cell differentiation also impacts cancer immunity. Increased expression of β-catenin in tumors is inversely correlated with intratumoral T-cell infiltration (11, 12).Tumor-intrinsic Wnt/β-catenin signaling mediates cancer immune evasion, by preventing T-cell or dendritic cell infiltration, migration and function, and resistance to immune checkpoint inhibitors (13–17). On the other hand, Wnt signaling is involved in the generation and maintenance of $CD8^+$ T-cell memory, by enabling intrinsic T-cell β-catenin accumulation and translocation into the nucleus, leading to a Tcf1-dependent expression of the Eomesodermin (EOMES) transcription factor (18–21). Gattinoni and colleagues showed that β-catenin signaling arrests $CD8^+$ T-effector cell differentiation, but promotes generation and maintenance of long-lived memory $CD8^+$ T cells with stem cell–like properties, defined as T stem cell memory because of their capacity to self-renew and supply waves of Teff cells on demand in both humans and mice (22, 23). T-cell–intrinsic β-catenin accumulation (due to GSK3β phosphorylation) leads to a Tcf1-dependent inhibition of interferon-γ (IFNγ) and nuclear transcription factors T-box (T-bet) transcription, resulting in inhibition of $CD4^+$ Th1-cell differentiation (24). Unresolved questions include the characterization of the microenvironments providing Wnt signals that, in turn, promote β-catenin accumulation in T cells and dampen $CD8^+$ Teff cell differentiation and enhance memory cells.

Here, we characterized $CD4^+$ and $CD8^+$ T cells infiltrating surgically excised tumor samples (from both HCC and colorectal cancer patients). We compared these T cells with their counterparts derived from nontumor tissue and peripheral blood (PB). We asked whether the tumor microenvironment (TME), in which both the cellular and secreted forms of Wnt3a are overexpressed (8, 9), may trigger downstream β-catenin signaling in $CD4^+$ or $CD8^+$ tumor-infiltrating T lymphocytes (TIL). In addition, we asked whether β-catenin signaling negatively conditions TIL-associated immune responses (25) or alters the differentiation and function of naïve T cells derived from healthy donors (HD).

Materials and Methods

Patients and cell purification

PB, nontumor, and tumor samples were obtained from HCC and colorectal cancer patients, not previously treated with chemotherapy. HCC patients were affected by hepatitis B virus (HBV) and/or hepatitis C virus (HCV) chronic hepatitis and carried cirrhosis at different stages. Patients' features are listed in Supplementary Table S1. Nontumor specimens were obtained in a distal zone compared with tumor specimens. Peripheral blood mononuclear cells (PBMC) were obtained from HCC and colorectal cancer patients by a density gradient, using Lympholyte (Cedarlane) and then collected in complete RPMI (Gibco) supplemented with 10% FBS (HyClone GE Healthcare Life Sciences), penicillin/streptomycin, nonessential amino acids, and sodium pyruvate (EuroClone) and 50 mol/L 2-mercaptoethanol (Sigma-Aldrich) and 2 mmol/L L-glutamine (Sigma-Aldrich). MCs were isolated from nontumor and tumor specimens from HCC and colorectal cancer patients. Tissue fragments were put in HBSS solution (Sigma-Aldrich; Ca/Mg) supplemented by 2% FBS (HyClone GE Healthcare Life Sciences), 0.5 mg/mL Collagenase IV (Sigma-Aldrich), 50 ng/mL DNA-si (Worthington, Ohio, USA) and 10% BSA (Thermo Fisher) in GentleMACS C tube, then by GentleMACS Octo Dissociator with Heaters (Miltenyi Biotec) "h_human_tumor 01_03" program was applied. The tissues were minced twice, with an interval of 10 minutes of incubation at 37°C between the first and second rounds. Cell suspension was obtained by disintegrating the fragments of tissue with a plunger of the syringe on cell strainer. Cell suspension was washed twice in cold HBSS (Sigma-Aldrich). MCs were pelleted with a 40% Percoll (GE Healthcare) solution, centrifuged in a Lympholyte (Cedarlane) gradient, and suspended in complete RPMI (Gibco; refs. 26, 27). Human studies were performed in accordance with the ethical guidelines of the 1975 Declaration of Helsinki and approved by the Institutional Ethical Committee (No. 3596). Written informed consent was obtained from all patients.

Tissue-conditioned media and serum samples

The tissue-conditioned media were obtained from nontumor and tumor tissue fragments of HCC or colorectal cancer patients by incubating small fragments of tissue in complete RPMI (Gibco) for 18 hours at 37°C (100 mg in 100 μL of complete RPMI). Serum samples were collected from 12 HCC, 9 colorectal cancer patients, and 6 HDs. The sera were obtained by the centrifugation (10′, 3000 RPM) of whole blood in serum tubes and then stored at −20°C before ELISA assay.

Flow cytometry

Antibodies (Ab) used in the study are listed in Supplementary Table S2. Dead cells in the cell suspension were excluded by adding Fixable-Viability Dye eFluor780 (eBioscience, Thermo Fisher) diluted in PBS 1X (EuroClone) for 30 minutes at room temperature (RT). Surface staining was performed by the incubation of MC enriched from PB, nontumor and tumor samples with selected Abs at 4°C for 20 minutes in PBS (EuroClone) 2% FBS (HyClone GE Healthcare Life Sciences). Intracellular staining of transcription factors was performed by using FOXP3 fixation and permeabilization buffer (eBioscience). To detect cytokine production, PBMCs and MCs were restimulated for 4 hours at 37°C with cell stimulation cocktail plus protein transport inhibitors (eBioscience). Samples were acquired on the BD LSRFortessa cell analyzer (BD Biosciences) and analyzed with FlowJo software, version 887 and 10.0.8r1 (TreeStar).

Functional assays

In vitro assays. $CD4^+CD45RA^+$ and $CD8^+CD45RA^+$ T naïve (TN) cells were isolated from PB of HDs by naïve $CD4^+$ T-cell isolation kit and naïve $CD8^+$ T-cell isolation kit (Miltenyi Biotec), respectively. The TN cell purity was checked by flow cytometry (FC) analysis resulting in 95% of $CCR7^+CD45RA^+$ in both $CD4^+$ and $CD8^+$ T cells. TN cells were cultured in complete RPMI medium (Gibco) in the presence of 100 U/mL of IL2 (Roche) and anti-CD3/CD28 Beads (Invitrogen, Thermo Fisher) at a 1:1 ratio. Either 5 μmol/L TWS119 (cat. number 3835; Tocris) or 400 ng/mL recombinant human Wnt3a (cat. number 5036-WN; R&D Systems) were added every day for 7 days. As control, cells were treated with 5 μmol/L DMSO (SERVA). At 72 hours or 7 days of culture, the expression of β-catenin, CCR7, CD45RA, T-bet,

Published OnlineFirst July 17, 2018; DOI: 10.1158/2326-6066.CIR-17-0712

Eomes, IFNγ, and TNFα was determined by surface and intracellular staining protocols of FC analysis. To detect cytokine production, T cells were restimulated for 4 hours at 37°C with cell stimulation cocktail plus protein transport inhibitors (eBioscience). In the same experiments, after overnight culture, we checked mRNA (AXIN2, TCF7) expression by real-time PCR, see details below. The experiments were performed in duplicate or in triplicate from single HDs; details are indicated in the figure legends. For each assay, 3 independent experiments were repeated.

Ex vivo assays. After enrichment of MC from nontumor and tumor samples, *ex vivo* assays were performed. Tumor-infiltrating MCs were cultured in complete RPMI (Gibco) in the presence of 100 U/mL of IL2 (Roche) and anti-CD3/CD28 Beads (Invitrogen) at the ratio 1:1 with the cells. In these conditions at days 3, 4, 5, and 6, 15 μg/mL anti-human/mouse Wnt3a (MAB1324; R&D Systems), or 15 μg/mL negative isotype control were added. In addition, 5 μmol/L TWS119 (cat. number 3835; Tocris) or DMSO (SERVA) were added every day, for 7 days. Then, β-catenin expression and TNFα production were assessed by surface and intracellular staining. To detect cytokine production, T cells were restimulated for 4 hours at 37°C with cell stimulation cocktail plus protein transport inhibitors (eBioscience).

Tissue-conditioned media and neutralization assays. $CD4^+CD45RA^+$ and $CD8^+CD45RA^+$ TN cells were isolated from PB of HDs as described above by a Miltenyi kit. $CD4^+CD45RA^+$ TN cells were cultured with tissue-conditioned media, obtained from nontumor and tumor fragments as described above, at different concentrations diluted in complete RPMI medium (1:10/1:100; Gibco), in the presence of anti-CD3/CD28 beads (Invitrogen) at a 1:1 ratio. After 7 days, β-catenin, T-bet, and Eomes expression were determined by FC analyses. Moreover, after 12 hours, mRNA from target genes (AXIN2 and TCF7) was analyzed by real-time PCR. To block the effects of soluble Wnt3a in the tissue-conditioned media, first we determined by ELISA kit (details below) that the amount of Wnt3a was around 50 to 60 ng/mL in the conditioned media derived from both nontumor and tumor tissues. $CD4^+CD45RA^+$ TN cells were stimulated with anti-CD3/CD28 Beads (Invitrogen; 1:1 ratio) in complete RPMI medium conditioned with 100 U/mL IL2 (Roche) for 7 days. At days 3, 4, 5, and 6, anti-human/mouse Wnt3a (MAB1324; R&D Systems; 15 μg/mL), or a negative isotype control (15 μg/mL) were added. After 7 days of culture, T-bet expression by FC analysis was analyzed. The neutralization assays were performed in duplicate, in 3 independent experiments.

Real-time PCR

mRNA target genes were analyzed from $CD4^+$ or $CD8^+$ TN cells after overnight culture with TWS119, rWnt3a, and after overnight culture with conditioned media. Total RNA was isolated from $CD4^+$ or $CD8^+$ T cells with the RNeasy Plus micro kit (Qiagen) according to the manufacturer's instructions. RNA was quantified by nano-photometer (IMPLEN) for each sample. DNA was reverse transcribed with high-capacity cDNA Reverse Transcription Kit (Thermo Fisher) according to the manufacturer's instructions. SYBR Green Master Mix (Thermo Fisher) was used for the amplification of target genes. Pairs of primers used are listed: CTNNB1: Forward 5′ GCACCACACCTTCTACAATGAGC 3′; Reverse 5′ TAGCACAGCCTGGATAGCAACG 3′; AXIN2 Forward 5′ AGCCAAAGCGATCTACAAAAGG 3′; Reverse 5′ GGTAGGCATTTTCCTCCATCAC 3′; TCF7 Forward 5′ GTGACAAAAGGCCCCTTTCCGAC 3′; Reverse 5′ CACAGGCCTGGCTGATTCCTTGT 3′. PCR reactions were run in Real-Time PCR StepOne (Applied Biosystems, Thermo Fisher). In order to quantify the data, the comparative Ct ($R = 2[CP\ sample - CP\ control]$ $R = 2\Delta CP$ and $R = 2-[\Delta CP\ sample - \Delta CP\ control]$ $R = 2-\Delta\Delta CP$) method was used. Relative quantity was defined as $2\text{-}\Delta\Delta Ct$, and β-actin (ACTB) was used as a reference gene.

ELISA

The concentration of Wnt3a levels were detected in conditioned media obtained from nontumor and tumor tissue fragments of HCC ($n = 33$) and colorectal cancer ($n = 9$) patients, as well as in the serum of HCC ($n = 12$) and colorectal cancer ($n = 9$) patients. As control, Wnt3a was also evaluated in the serum of 6 HDs. ELISA was performed according to the manufacture's instruction of Cloud Clone Corp kit or to the manufacturer's instruction of Human Protein Wnt3a ELISA kit (Cat. CSB-EL026136HU, Cusabio Technology).

Statistical analysis

Statistical analysis was performed using Prism software (version 6.0c, GraphPad). *Ex vivo* data were analyzed by Wilcoxon matched-pairs test, two-tailed or paired matched *t* test, two-tailed. Mann–Whitney test, two-tailed, was applied to analyze Wnt3a concentration by ELISA assay. For *in vitro* assays, we used the Student *t* test. The Spearman test was used for the correlations between biological parameters. $P < 0.05$ was considered statistically significant in all tests.

Results

Effector TILs from HCC and colorectal cancer express a partially exhausted phenotype

First, we used FC to analyze the activation markers CD69 and programmed death (PD)-1, a receptor expressed by activated T cells that delivers a negative signal, leading to exhaustion particularly in $CD8^+$ T cells (28). Both markers were upregulated by both $CD4^+$ or $CD8^+$ T cells infiltrating nontumor and tumor districts, as compared with their peripheral counterparts, in HCC (Fig. 1A–D) and colorectal cancer (Supplementary Fig. S1A and S1B) patients. The majority of these tissue-infiltrating T cells expressed an effector memory (EM; $CCR7^-CD45RA^-$), as compared with terminal effector memory RA^+ (EMRA; $CCR7^-RA^+$), or central memory (CM; $CCR7^+CD45RA^-$) phenotype (Fig. 1E–G; Supplementary Fig. S1C and S1D). In contrast, $CD4^+$ and $CD8^+$ TEMRA cells tended to decrease in tumor districts, suggesting that the tumor microenvironment may perturb differentiation of T cells with terminal effector functions. Despite the PD-1 expression, these cells were not fully exhausted (28). Indeed, neither tumor-infiltrating $CD4^+$ nor $CD8^+$ T cells lost the capacity to produce IFNγ and tumor necrosis factor (TNF)-α or to degranulate [as detected by the mobilization of CD107a, a lysosomal associated membrane protein-1 (29), to the cell membrane], in response to few hours of contact with polyclonal stimuli, as compared with the peripheral or nontumor counterparts (Fig. 2A–H). IFNγ and TNFα production was not inversely related with the PD-1 expression, supporting the idea that PD-1 expression is not associated with a complete dysfunction/exhaustion of these cells (Fig. 2I and J). By analyzing the expression of T-bet and

Published OnlineFirst July 17, 2018; DOI: 10.1158/2326-6066.CIR-17-0712

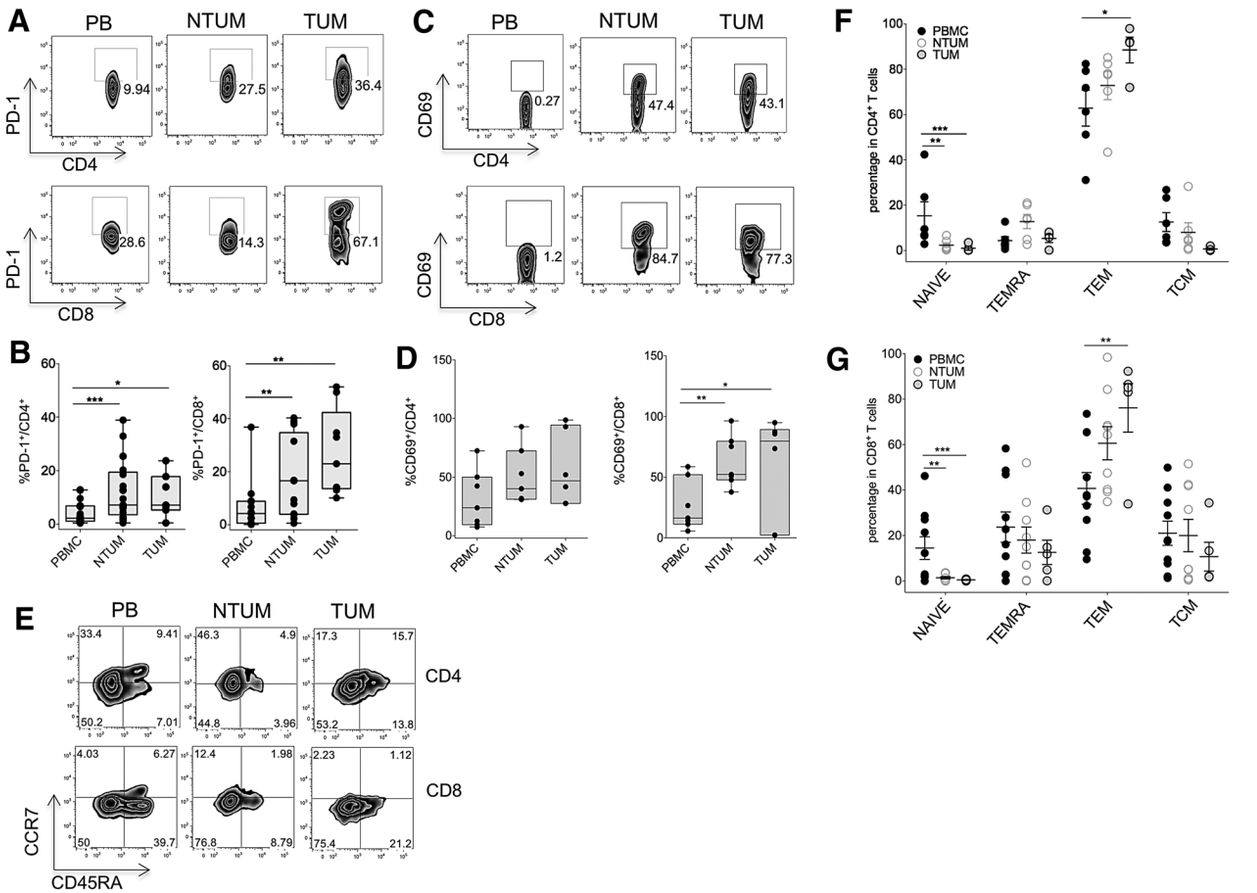

Figure 1.

$CD4^+$ and CD8 T^+ cells expressed PD1 in tumor district and showed an EM phenotype in HCC. **A,** Representative PD-1 expression by FC analysis of $CD4^+$ and $CD8^+$ T cells in PB, nontumor (NTUM), and tumor (TUM) districts of HCC patients. **B,** Percentage of $PD1^+$ $CD4^+$ and $CD8^+$ T cells in PB, NTUM, and TUM specimens of HCC patients. PB, NTUM, and TUM ($n = 24$). *, $P < 0.05$; **, $P < 0.01$; ***, $P < 0.005$, paired matched *t* test two-tailed between different districts (PB, NTUM, TUM) of the same patient. **C,** Representative CD69 expression by FC analysis of $CD4^+$ and $CD8^+$ T cells in PB, NTUM, and TUM districts of HCC patients. **D,** Percentage of $CD69^+$ $CD4^+$ and $CD8^+$ T cells in PB, NTUM, and TUM specimens of HCC patients. PB, NTUM, and TUM ($n = 8$). *, $P < 0.05$; **, $P < 0.01$, paired matched *t* test two-tailed between different districts (PB, NTUM, TUM) of the same patient. **E,** Representative CCR7/CD45RA expression in both $CD4^+$ and $CD8^+$ T-cell subset by FC analysis in PB, NTUM, and TUM of HCC patients. **F** and **G,** Percentage of naïve ($CCR7^+CD45RA^+$), TEMRA ($CCR7^-CD45RA^+$), TEM ($CCR7^-CD45RA^-$), and TCM ($CCR7^+$ $CD45RA^-$) within $CD4^+$ and CD^+8 T-cell subset in PB, NTUM, and TUM districts of HCC patients ($n = 10$). *, $P < 0.05$; **, $P < 0.01$; ***, $P < 0.005$, Wilcoxon matched-pairs test, two-tailed.

Eomes, which allowed us to identify $CD8^+$ Teff cells as either functional $Eomes^+T\text{-}bet^+$ or dysfunctional $Eomes^+T\text{-}bet^-$ cells (28), we found that $CD4^+$ and $CD8^+$ Teff cell populations expressing $Eomes^+T\text{-}bet^+$ or $Eomes^+T\text{-}bet^-$ phenotype coexisted in both nontumor and tumor districts, indicating that Teff cells are not widely dysfunctional in these tumor microenvironments (Fig. 3A–E). Similar observations are reported in the non–small cell lung cancer setting (26). We found no difference in these T-cell subsets between HBV- or HCV-related HCC or among different HCC or colorectal cancer tumor stages.

β-Catenin expression marks TILs with a partially exhausted phenotype

We wondered if β-catenin expression was upregulated in nontumor- and tumor-infiltrating T cells, and if the cellular or secreted forms of Wnt3a (8, 9), might trigger downstream β-catenin signaling into TILs. Wnt3a was significantly represented in conditioned media from nontumor and tumor tissues (derived from liver and colon tissue fragments of both HCC and colorectal cancer patients; Fig. 4A and B; Supplementary Fig. S2A and S2B). The circulating serum Wnt3a concentrations were significantly lower than those found in conditioned media from nontumor and tumor tissues, suggesting that the serum Wnt3a does not reflect the real synthesis of Wnt3a occurring *in situ* (Fig. 4A; Supplementary Fig. S2A and S2B). The Wnt3a levels in conditioned media tended to be higher in the stage I and/or II of tumors, calculated according to the TNM classification (Fig. 4B; ref. 30). β-Catenin expression, calculated as mean fluorescence intensity (MFI), was significantly upregulated in $CD4^+$ and $CD8^+$ T cells infiltrating both nontumor and tumor tissues, whereas Wnt3a expression was significantly upregulated in nontumor-infiltrating T cells, as compared with peripheral counterparts (Fig. 4C–F; Supplementary Fig. S2C–S2F). β-Catenin was directly correlated with Wnt3a expression in both tumor-infiltrating and

Published OnlineFirst July 17, 2018; DOI: 10.1158/2326-6066.CIR-17-0712

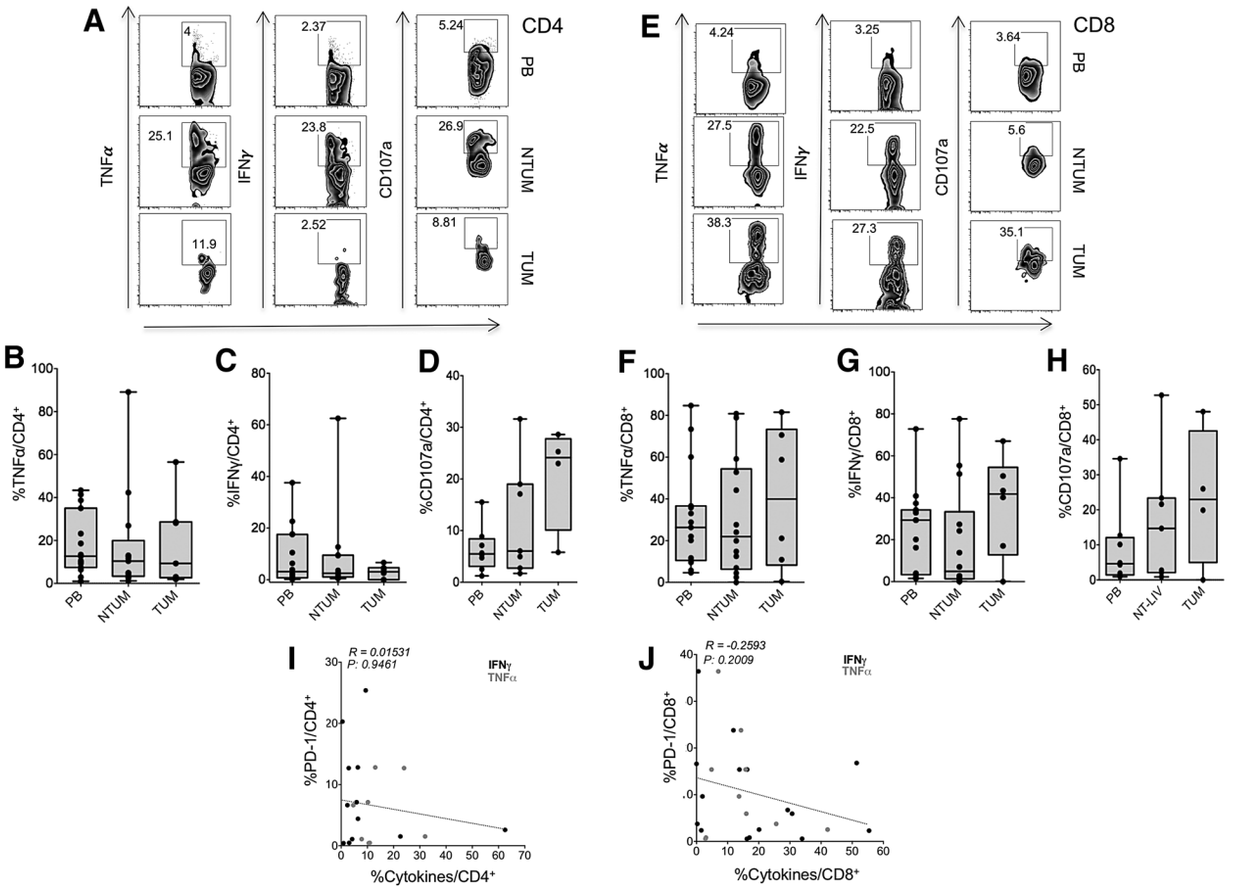

Figure 2.

$CD4^+$ and $CD8^+$ T cells produced IFNγ and TNFα and expressed CD107a in tumor samples of HCC. **A,** Representative TNFα, IFNγ, and CD107a expression by FC analysis of $CD4^+$ T cells in PB, nontumor (NTUM), and tumor (TUM) districts of HCC patients. **B–D,** Percentage of $TNF\alpha^+$, $IFN\gamma^+$, and $CD107a^+$ cells in gated $CD4^+$ T cells in PB, NTUM, and TUM specimens of HCC patients ($n = 20$). **E,** Representative TNFα, IFNγ, and CD107a expression by FC analysis of $CD8^+$ T cells in PB, NTUM, and TUM districts of HCC patients. **F–H,** Percentage of $TNF\alpha^+$, $IFN\gamma^+$, and $CD107a^+$ in gated $CD8^+$ T cells in PB, NTUM, and TUM specimens of HCC patients ($n = 20$). **I** and **J,** Spearman correlations between the percentage of PD-1^+ $CD4^+$ ($n = 11$) and $CD8^+$ ($n = 17$) T cells and the percentage of $IFN\gamma^+$ and $TNF\alpha^+$ $CD4^+$ and $CD8^+$ T cells. The correlation data derived from all pooled districts (PB, NTUM, and TUM).

noninfiltrating $CD4^+$ and $CD8^+$ T cells, proposing a possible cause-and-effect relationship between these events (Fig. 4E–G). In contrast, no correlation was observed between β-catenin expression by infiltrating $CD4^+$ or $CD8^+$ T cells and the serum or secreted form of Wnt3a detected in conditioned media from nontumor and tumor tissues. β-Catenin and Wnt3a expression in both nontumor and tumor-derived $CD4^+$ or $CD8^+$ T cells tended to be higher in stage I tumors (Fig. 4H; Supplementary Fig. S2F). No difference was revealed for FzdR1 (Supplementary Fig. S3A–S3C). β-$Catenin^+$ cells were more prevalent among $Eomes^+$T-bet^- cells, which are effector cells with a dysfunctional phenotype (28), as compared with the $Eomes^+$T-bet^+ cells (Fig. 5A and B). As a consequence, $Eomes^+$T-bet^- cells were more concentrated within the β-$catenin^+$ cell population than within the β-$catenin^-$ cell population in both $CD4^+$ or $CD8^+$ Teff cells from nontumor and tumor districts (Fig. 5C and D). β-Catenin expression correlated with the frequency of cells with $Eomes^+$T-bet^- phenotype (Fig. 5E and F), but not with the frequency of TILs producing IFNγ (Fig. 5G). By contrast, β-catenin expression was similar in $CD4^+$ or $CD8^+$ T cells that did or did not express PD-1 in nontumor and tumor districts and in the periphery (Fig. 5H).

Wnt3a activates β-catenin signaling allowing a partially exhausted phenotype in T cells

Then, we performed a series of experiments *in vitro* and *ex vivo* to provide a mechanistic support for the hypothesis that Wnt3a signaling may condition the phenotype observed for nontumor or tumor-infiltrating Teff cells (i.e., $Eomes^{high}$T-bet^{low}β-$catenin^{high}$). First, we added TWS119, which inhibits GSK3b in the β-catenin destruction complex (23), at the start of a culture in which purified ($CCR7^+CD45RA^+$) $CD4^+$ TN cells were stimulated with anti-CD3/anti-CD28 for 72 hours or 7 days. Under these conditions, β-catenin was significantly upregulated and mRNA of both AXIN2 and TCF7 (prominent target genes of β-catenin) was overexpressed in the resulting differentiated T cells (Fig. 6A and B). Some of the resulting T cells that expressed β-catenin retained the expression of CCR7 and downregulated CD45RA, acquiring thus a CM phenotype. Other of these T cells acquired an effector

Published OnlineFirst July 17, 2018; DOI: 10.1158/2326-6066.CIR-17-0712

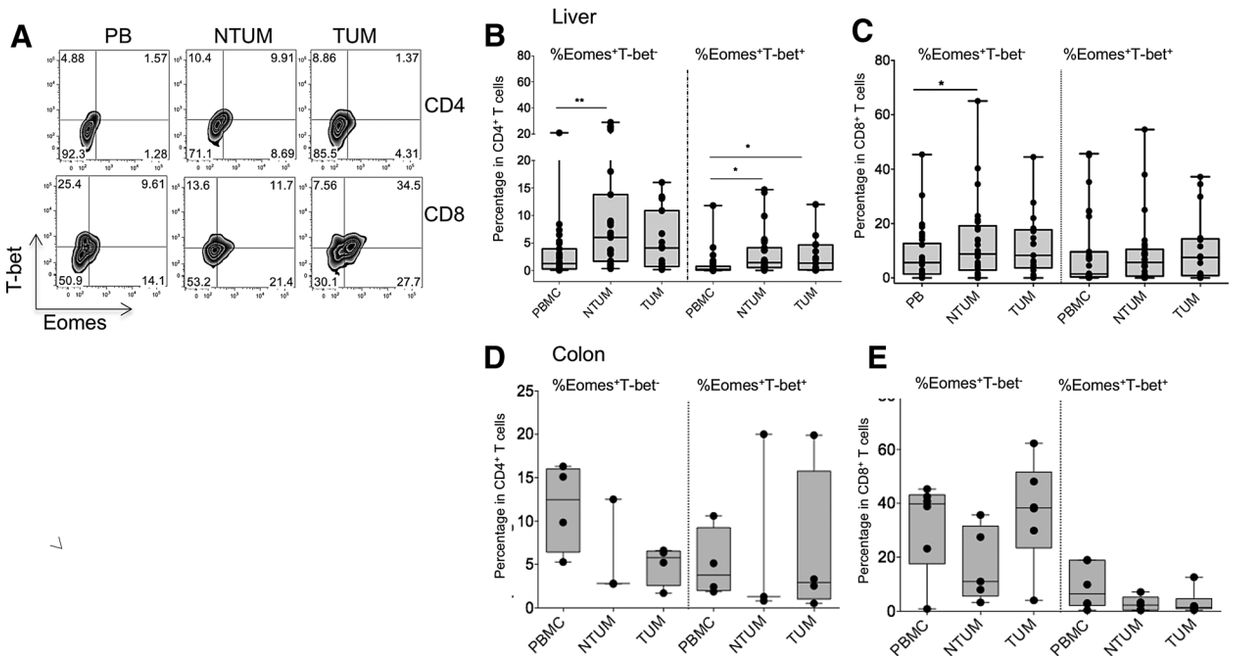

Figure 3.

Distribution of Eomes$^+$T-bet$^-$ and Eomes$^+$T-bet$^+$ CD4$^+$ and CD8$^+$ T-cell subsets in PB, nontumor, and tumor samples of HCC and colorectal cancer patients. **A,** Representative T-bet/Eomes expression by FC analysis in both CD4$^+$ and CD8$^+$ T-cell subsets in PB, nontumor (NTUM), and tumor (TUM) districts of HCC patients. **B** and **C,** Percentage of Eomes$^+$T-bet$^-$ and Eomes$^-$T-bet$^+$ in both CD4$^+$ and CD8$^+$ T-cell subsets in PB, NTUM and TUM samples of HCC patients ($n = 24$). *, $P < 0.05$; **, $P < 0.01$, paired matched t test two-tailed between different districts (PB, NTUM, TUM) of the same patient. **D** and **E,** Percentage of Eomes$^+$T-bet$^-$ and Eomes$^-$T-bet$^+$ in both CD4$^+$ and CD8$^+$ T-cell subsets in PB, NTUM, and TUM samples of colorectal cancer patients ($n = 8$).

CCR7$^-$CD45RA$^-$ phenotype (Fig. 6C and D). Cells that lacked β-catenin maintained a naïve CCR7$^+$CD45RA$^+$ phenotype (Fig. 6D). β-Catenin upregulation in *in vitro*–differentiated T cells was associated with a consistent downregulation of T-bet expression after TWS119 treatment culture (Fig. 6E and F). Eomes expression was not affected (Fig. 6E and F), confirming the distribution of β-catenin expression shown within nontumor or tumor-infiltrating Teff cells *in vivo*. Similar results were obtained in conditions in which CCR7$^+$CD45RA$^+$ TN cells were stimulated in the presence of a recombinant form of Wnt3a (rWnt3a; a FdzR agonist): indeed, the resulting differentiated T cells upregulated β-catenin and downregulated T-bet in the presence of rWnt3a, as compared with those stimulated without the addition of rWnt3a (Fig. 6G and H). To confirm that T-bet downregulation, obtained upon Wnt/β-catenin signaling, perturbed effector T-cell functions, we assessed IFNγ or TNFα production in the presence or absence of rWnt3a *in vitro*. The treatment of TN cells with rWnt3a significantly downregulated the differentiation into cells producing IFNγ or TNFα (Fig. 6I). Similar results were obtained with CD8$^+$ T cells. To explore whether TWS119 or rWnt3a might also affect tumor microenvironments, we measured the capacity of conditioned media containing Wnt3a from HCC or colorectal cancer tissue samples to condition T-cell differentiation. In the same experimental setting, Wnt3a$^+$-conditioned media from nontumor or tumor tissues (but not conditioned media from cultured PBMCs in which secreted Wnt3a was undetectable), when added to purified CD4$^+$CD45RA$^+$ TN cells in the presence of anti-CD3/anti-CD28, recapitulated the effects of TWS119 or rWnt3a. Indeed, the resulting differentiated T cells upregulated the expression of β-catenin, as well as of the β-catenin mRNA targets AXIN2 and TCF7, and downregulated the expression of T-bet, but not of Eomes (Fig. 7A–G). To validate the involvement of Wnt3a-containing conditioned media in supporting the acquisition of a partially exhausted phenotype by T cells, we added in the same experiments, in which purified CD4$^+$CD45RA$^+$ TN cells were stimulated in the presence of Wnt3a$^+$-conditioned media, a neutralizing anti-Wnt3a. In this experimental setting, we observed a significant, increase of T-bet expression in differentiated T cells (Fig. 7H). To verify if the neutralizing anti-Wnt3a mAb might restore the partially exhausted phenotype observed in β-catenin–expressing tumor-infiltrating Teff cells (see Figs. 3 and 4), both nontumor or tumor-isolated experienced T cells were stimulated in the presence of anti-Wnt3a for 24 hours. The addition of anti-Wnt3a to the culture, in which purified β-catenin$^+$ nontumor or tumor-derived T cells were stimulated in the presence of Wnt3a$^+$-conditioned media, did not improve the effector function of these cells *ex vivo*, in terms of IFNγ or TNFα production, CD107a mobilization, or T-bet, Eomes, or PD-1 expression (Supplementary Fig. S4).

Discussion

TILs exert clinically relevant pressure against tumor progression likely due to the somatically mutated (nonself) neoepitopes generated in tumor cells (25, 31–33). However, after equilibrium between tumor progression and immune surveillance, antitumor immunity loses effector functions, in part because of the emergence of inhibitory signaling pathways (called immune

Published OnlineFirst July 17, 2018; DOI: 10.1158/2326-6066.CIR-17-0712

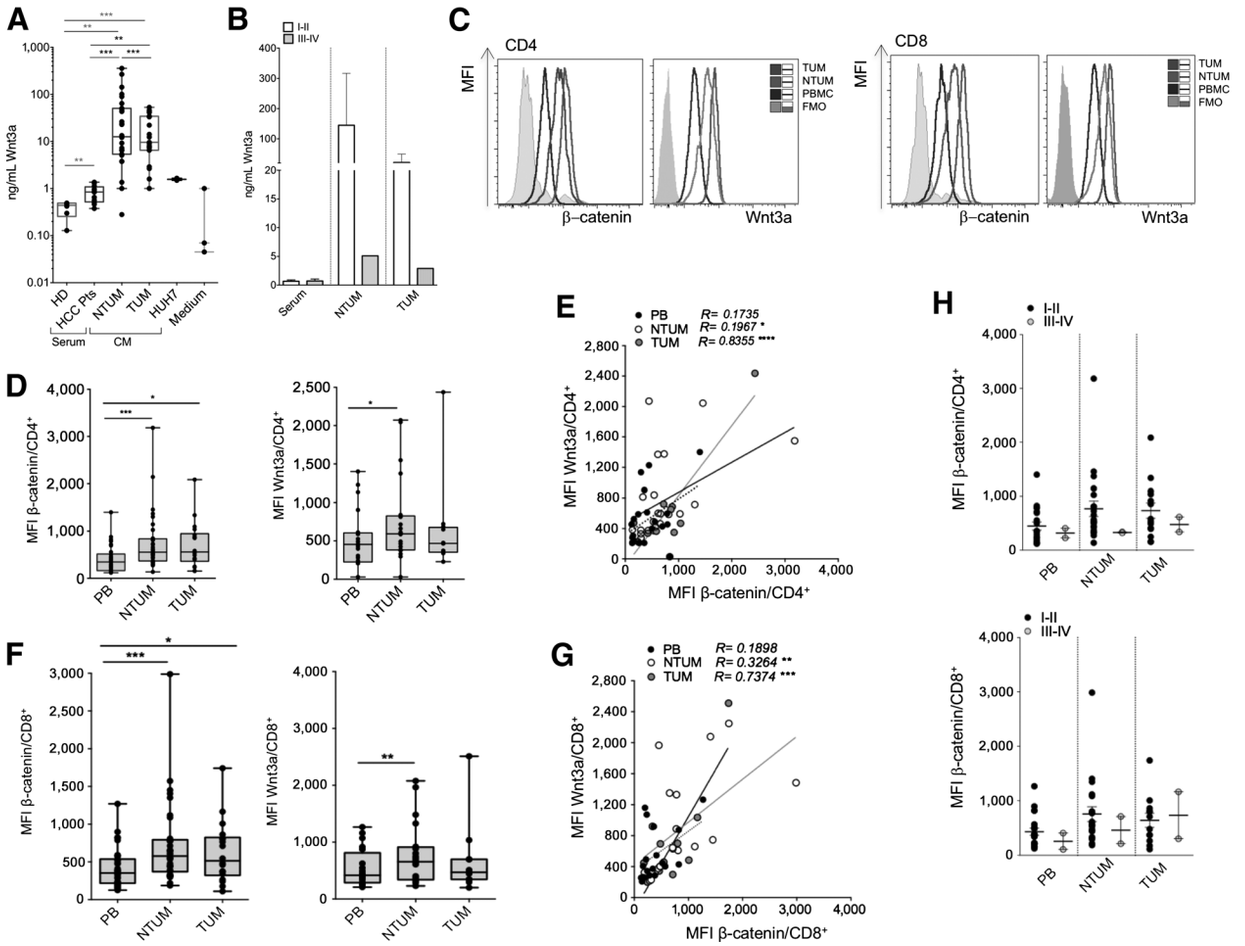

Figure 4.

Distribution of Wnt3a in serum nontumor- or tumor-derived conditioned media and expression of the Wnt3a/β-catenin axis in nontumor and tumor-infiltrating CD4$^+$ and CD8$^+$ T cells from HCC patients. **A,** Wnt3a levels, as evaluated by ELISA in serum from 6 HDs and 12 HCC patients (pts), in conditioned medium from nontumor (NTUM) and tumor (TUM) tissue fragments derived from HCC patients ($n = 12$), in conditioned media from commercial HUH7 cell line, and in the complete RPMI medium; **, $P < 0.01$; ***, $P < 0.005$, Mann–Whitney test, two-tailed between HD and HCC patients sera; **, $P < 0.01$; ***, $P < 0.005$; Wilcoxon matched-pairs among HCC samples (serum HCC pts, NTUM-, and TUM-derived conditioned media). **B,** Wnt3a determined in HCC patients' serum or conditioned media from NTUM and TUM tissue fragments were stratified according to TNM classification (I–II stage vs. III–IV stage). **C,** Representative MFI of β-catenin and Wnt3a in CD4$^+$ or CD8$^+$ T cells isolated from PB, NTUM, and TUM samples of a HCC patient. **D,** The graphs show the MFI of β-catenin and Wnt3a in PB-, NTUM-, or TUM-derived CD4$^+$ T cells from 30 HCC patients. *, $P < 0.05$; ***, $P < 0.005$, paired matched t test two-tailed between different districts (PB, NTUM, and TUM) of the same patient. **F,** The graphs show the MFI of β-catenin and Wnt3a in PB-, NTUM-, or TUM-derived CD8$^+$ T cells from 30 HCC patients. *, $P < 0.05$; **, $P < 0.01$; ***, $P < 0.005$, paired matched t test two-tailed between different districts (PB, NTUM, and TUM) of the same patient. **E–G,** Spearman correlations between MFI of Wnt3a and β-catenin in PB-, NTUM-, or TUM-derived CD4$^+$ (**E**) or CD8$^+$ (**G**) T cells from 20 HCC patients. *, $P < 0.05$; **, $P < 0.01$; ***, $P < 0.005$; ****, $P < 0.0001$. **H,** MFI of β-catenin in both CD4$^+$ and CD8$^+$ T cells derived from PB, NTUM, and TUM specimens of 30 HCC patients, stratified according to TNM classification (I–II stage vs. III–IV stage).

checkpoints, such as PD-1 or CTLA-4; refs. 25, 34). Immunotherapy using mAbs specific to immune checkpoints, defined as inhibitory checkpoints (e.g., anti-PD-1 or anti-CTLA-4), has been shown to be efficacious in some but not all tumor patients (35, 36), likely due to failure of the mechanisms maintaining tumor dormancy (25) and establishment of T-cell exhaustion (28). Eomes$^+$T-bet$^+$ and Eomes$^+$T-bet$^-$ cell phenotypes discriminate functional and dysfunctional T cells, respectively. Eomes$^+$T-bet$^-$ cells expressing PD-1^{low} are partially dysfunctional or exhausted and can be rescued by blockade of the PD-1 pathway. Fully exhausted Eomes$^+$T-bet$^-$PD-1^{high} cells cannot (28). Some Teff (EM) cells from HCC and colorectal cancer expressed a partially exhausted phenotype, because they were able to produce IFNγ and TNFα despite the PD-1 expression.

We suggest that β-catenin upregulation in Teff cells (EM or EMRA cells representing the most abundant nontumor- or tumor-infiltrating populations) marks the partially exhausted Eomes$^+$T-bet$^-$PD-1$^{-/+}$ cells that previous reports have shown to be susceptible to PD-1 blockade (28). This hypothesis is consistent with data showing that CD8$^+$ T cells expressing the β-catenin target TCF7 and exhibiting features intermediate between CM and exhausted T cells expand upon immune checkpoint blockade (37). Expression of β-catenin was correlated with intrinsic Wnt3a expression in infiltrating CD4$^+$ and CD8$^+$ T cells (particularly in

Published OnlineFirst July 17, 2018; DOI: 10.1158/2326-6066.CIR-17-0712

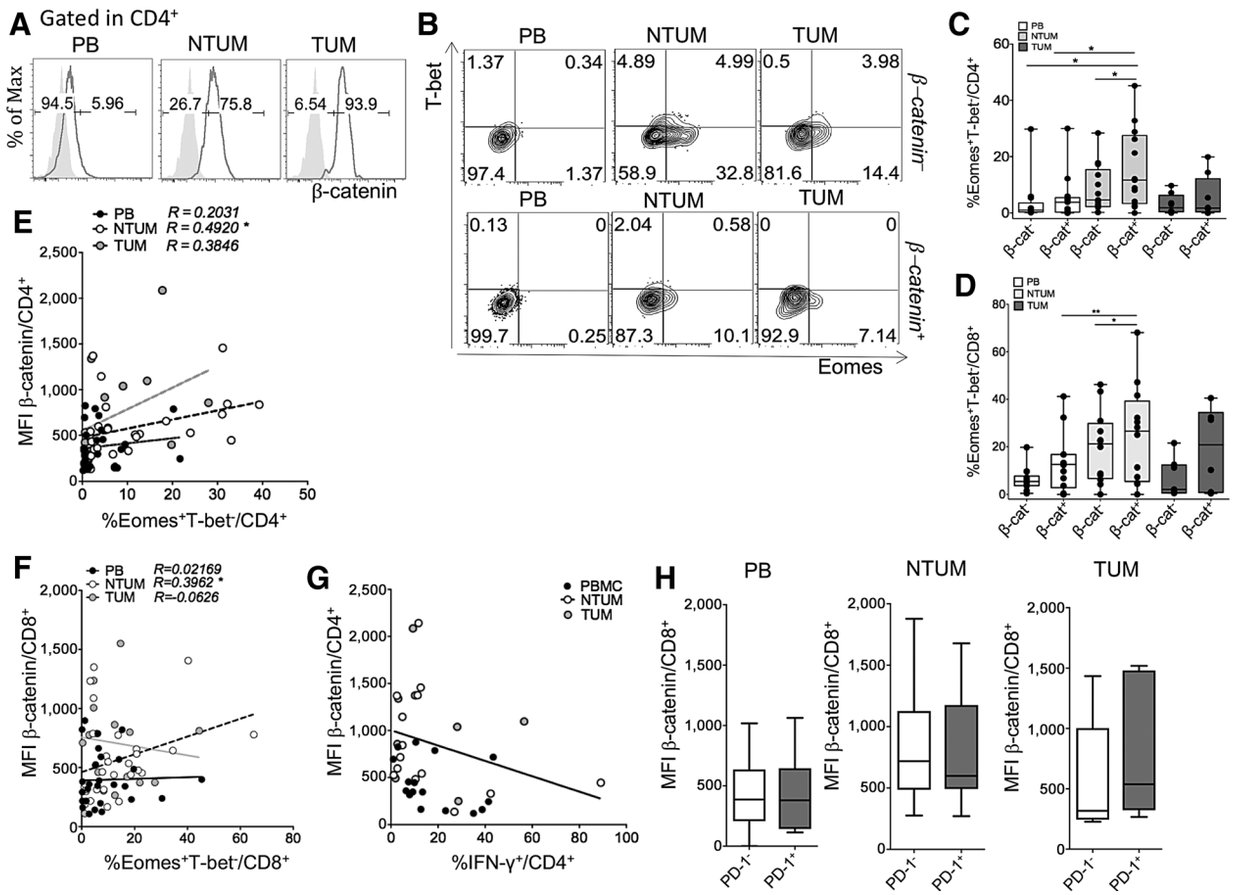

Figure 5.

β-Catenin$^+$ CD4$^+$ and CD8$^+$ T cells were more represented in the Eomes$^+$T-bet$^-$ T-cell subset. **A** and **B,** Representative MFI of β-catenin in PB, nontumor (NTUM), and (TUM) samples of HCC patients in gated CD4$^+$ T cells and representative T-bet/Eomes expression by FC analysis within β-catenin$^+$ versus β-catenin$^-$ gated in CD4 T cells, in PB, NTUM, and TUM samples of HCC patients. **C** and **D,** The graphs showed the percentage of Eomes$^+$T-bet$^-$ of CD4$^+$ and CD8$^+$ T-cell subsets within β-catenin$^+$ versus β-catenin$^-$ T cells in PB, NTUM, and TUM specimens of HCC patients. PB, NTUM, and TUM ($n = 20$). *, $P < 0.05$; **, $P < 0.01$, paired matched *t* test two-tailed between different districts (PB, NTUM, and TUM) of the same patient and Wilcoxon matched-pairs test, two-tailed. **E** and **F,** Spearman correlations between MFI of β-catenin and frequency of Eomes$^+$T-bet$^-$ gated in both CD4$^+$ and CD8$^+$ T cells of HCC patients. PB, NTUM, and TUM ($n = 20$). *, $P < 0.05$. **G,** Spearman correlation between MFI of β-catenin and percentage of IFNγ$^+$ CD4 T cells in PB, NTUM, and TUM of HCC patients. The linear regression indicated NTUM compartment. PB, NTUM, and TUM ($n = 20$). **H,** The graphs showed the MFI of β-catenin within PD1$^+$ versus PD1$^-$ CD$^+$8 T-cell subsets in PB, NTUM, and TUM of HCC patients.

the tumor district), but not with Wnt3a expression in serum levels or in conditioned media from nontumor or tumor tissues. We therefore suggest that an autocrine loop may maintain Wnt/β-catenin signaling in TILs, and the Wnt3a secreted by tumor or stromal cells is redundant. The evidence that β-catenin$^+$PD-1$^{-/+}$ Teff cells (previously reported to be partially exhausted cells that can be rescued by blockade of the PD-1 pathway; refs. 28 and 37), as well as the secreted form of Wnt3a, were prominent in stage I tumors is consistent with the hypothesis that β-catenin$^+$PD-1$^{-/+}$ Teff cells might be rescued from a progression toward exhaustion by PD-1 blockade in the early phase of tumors. However, CD4$^+$ or CD8$^+$ TCM cells trapped in draining lymphoid tissues may upregulate β-catenin expression, consistent with reports that Wnt/β-catenin signaling generates and maintains CD8$^+$ T-cell memory (18–21, 38) by arresting cell differentiation (22, 23).

No phenotypic or functional difference was observed between nontumor or tumor-derived T cells: both expressed a similar partially exhausted phenotype (Eomes$^+$T-bet$^-$PD-1$^{-/+}$ IFNγ$^+$ TNFα$^+$) and similar β-catenin expression. Wnt3a expression in nontumor or tumor-derived T cells may deliver β-catenin–dependent signals that could generate T cells with a partially exhausted phenotype, a cell type instrumental in establishing chronic low-level inflammation that promotes the tumor program.

To determine whether Wnt3a/β-catenin signaling affects differentiation of TN cells, we examined the effects of TWS119, rWnt3a, or conditioned media from HCC or colorectal cancer containing Wnt3a *in vitro* or *ex vivo*. Indeed, TN cells stimulated in the presence of TWS119, rWnt3a, or Wnt3a$^+$-conditioned media *in vitro* differentiated into T cells with either a CM or a TEM phenotype, in which expression of β-catenin and β-catenin targets AXIN2 and TCF7 were upregulated, T-bet was downregulated, Eomes expression was unaffected, and IFNγ or TNFα production was only partially downregulated. Thus, the Teff cells generated

Published OnlineFirst July 17, 2018; DOI: 10.1158/2326-6066.CIR-17-0712

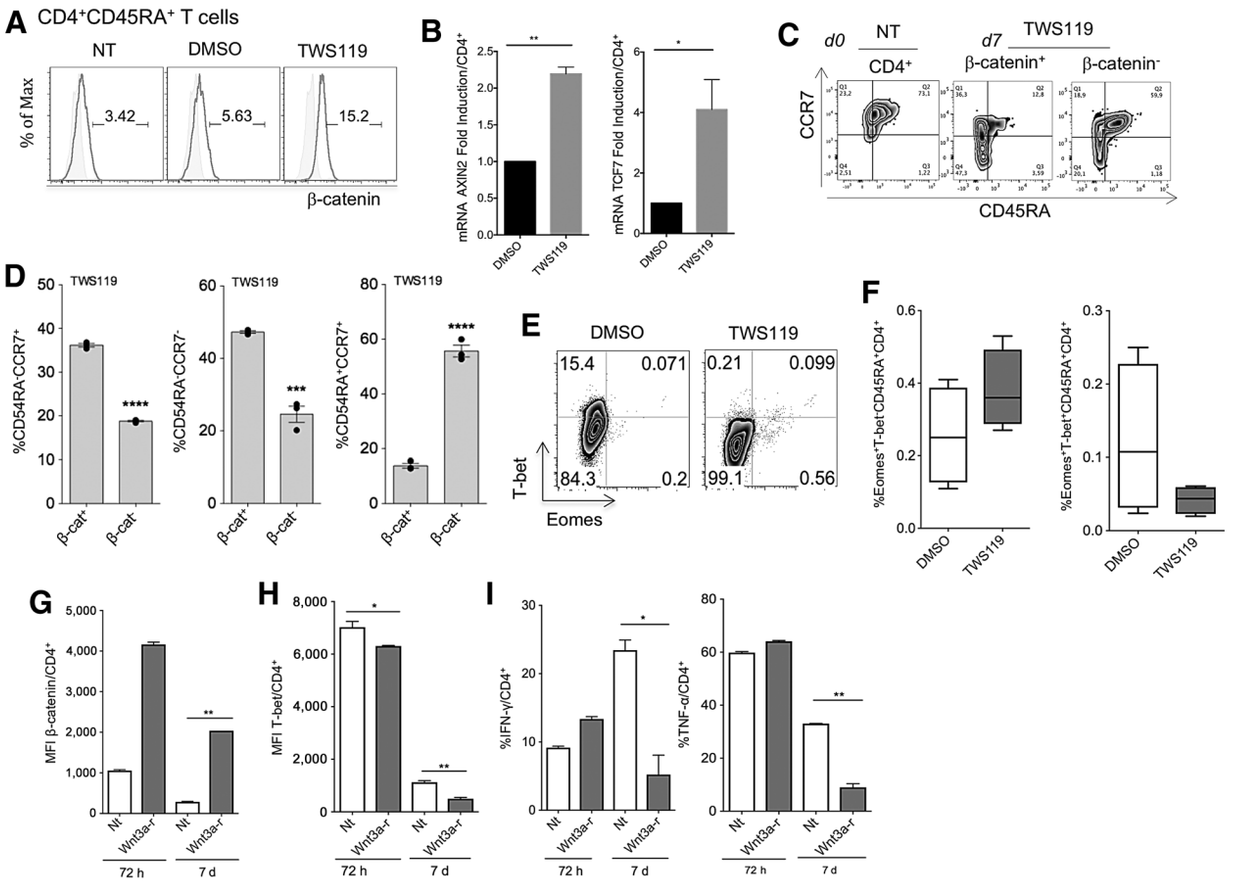

Figure 6.

CD4$^+$CD45RA$^+$ TN cells in the presence of TWS119 and rWnt3a upregulated β-catenin and decreased T-bet expression. **A,** Representative MFI of β-catenin in gated CD4 T-cell subset after CD4$^+$CD45RA$^+$ TN cell culture of 7 days with TWS119 (5 μmol/L). **B,** mRNA expression of AXIN2 and TCF7 was evaluated at day 1 by real-time PCR in CD4$^+$CD45RA$^+$ TN cells after 7 days of TWS119 (5 μmol/L) culture. The graphs showed a representative experiment ($n = 2$) out of 3 showing similar results. *, $P < 0.05$; **, $P < 0.01$, Student t test. **C,** Representative CCR7/CD45RA expression by FC within CD4$^+$ T-cell subset at day 0 in NT samples and within β-catenin$^+$ versus β-catenin$^-$ CD4$^+$ T cells after 7 days of TWS119 (5 μmol/L) culture. **D,** The graphs showed the percentage of CM (CCR7$^+$CD45RA$^-$) and EM (CCR7$^-$CD45RA$^-$) and naïve (CCR7$^+$CD45RA$^+$) CD4 T cells within β-catenin$^+$ versus β-catenin$^-$ CD4 T cells, after 7 days of TWS119 (5 μmol/L) culture. The graphs showed 1 representative experiment ($n = 3$) out of 3 independent experiments. ***, $P < 0.005$; ****, $P < 0.0001$, Student t test. **E,** Representative T-bet/Eomes expression by FC analysis within CD4$^+$ T-cell subpopulation, after day 7 of CD4$^+$CD45RA$^+$ TN cell culture with DMSO (5 μmol/L) and TWS119 (5 μmol/L). **F,** The graphs indicated the percentage of Eomes$^+$T-bet$^-$ and Eomes$^+$T-bet$^+$ within CD4 T-cell subset after 7 days of CD4$^+$CD45RA$^+$ TN cell culture with TWS119 (5 μmol/L) compared with DMSO (5 μmol/L), as control. The graphs showed a representative experiment ($n = 2$) out of 3 showing similar results. **G,** MFI of β-catenin in the gated CD4 T-cell subpopulation after CD4$^+$CD45RA$^+$ TN cell culture of 72 hours and 7 days with rWnt3a (400 ng/mL) compared with nontreated (NT) samples. The graph presented a representative experiment ($n = 2$) out of 3, showing similar results. **, $P < 0.01$, Student t test. **H** and **I,** The graph displayed the MFI of T-bet and the percentage of IFNγ and TNFα producers CD4 T cells observed in *in vitro* culture of CD4$^+$CD45RA$^+$ TN cells treated with rWNt3a (400 ng/mL) at 72 hours and 7 days. The graphs indicated 1 representative experiment of 2 HD out of 3 independent experiments. *, $P < 0.05$; **, $P < 0.01$, Student t test.

after stabilization of β-catenin *in vitro* were arrested at a stage similar to cells that infiltrate the tumor or peritumor areas *in vivo*. These Eomes^{high}T-bet^{low}PD-1$^+$β-catenin^{high} Teff cells with moderate effector functions (partially exhausted) were, however, unable to eradicate the tumor. Our results suggest that Wnt3a/β-catenin signaling promoted the generation and maintenance of CD8$^+$ T-cell memory from TN cells (18–21, 38), at the expense of differentiation of Teff cells (22–24). Such partially differentiated cells may sustain a long period of immune surveillance with their moderate capacity to perform effector-cell functions.

When T-cell differentiation from TN cells was affected by the addition of Wnt3a$^+$-conditioned media *in vitro*, concurrent addition of a neutralizing anti-Wnt3a partially restored T-bet expression in differentiated T cells. Thus, Wnt3a secreted in the tumor microenvironment impairs T-cell differentiation. Other factors in the tumor microenvironment may also be involved. Studies are in progress to address this issue by analyzing the tumor secretome through mass spectrometry and proteomics. We asked whether a negative loop between Wnt3a and β-catenin, which were simultaneously expressed by nontumor or tumor-infiltrating Teff cells, might be interrupted by the addition of a neutralizing anti-Wnt3a. We found no improvement of effector function or T-bet expression by these cells. We conclude that Wnt/β-catenin signaling arrests differentiation of TN cells into effector cells but does not affect function and phenotype of well-differentiated T cells. However, the blockade of Wnt/β-catenin signaling

Published OnlineFirst July 17, 2018; DOI: 10.1158/2326-6066.CIR-17-0712

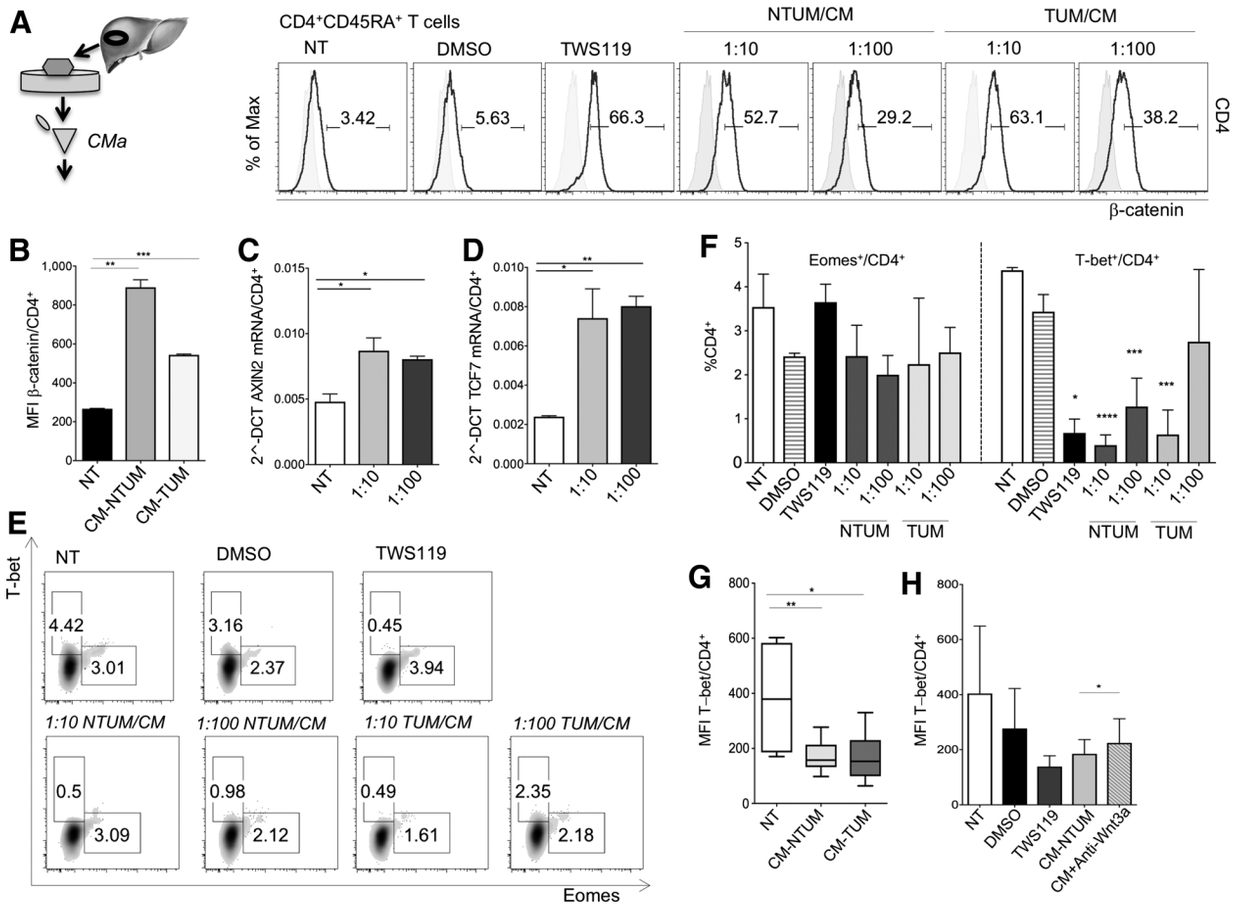

Figure 7.

$CD4^+CD45RA^+$ TN cells cultured with conditioned media from nontumor and tumor (of HCC tissue fragments) recapitulated TWS119 and rWnt3a effects *in vitro* by decreasing T-bet expression. **A,** Representative experiment showing the MFI of β-catenin within $CD4^+$ T-cell subpopulation. $CD4^+CD45RA^+$ TN cells were cultured for 7 days with conditioned media at the concentration of 1:10/1:100 in complete RPMI and are included in the experiment TWS119 (5 μmol/L) and DMSO (5 μmol/L), as controls. **B,** The graph showed the MFI of β-catenin within $CD4^+$ T-cell subset after 7 days of $CD4^+CD45RA^+$ TN cell culture with conditioned media (generated from NTUM and TUM liver tissue fragments) compared with medium (NT). The graph showed 1 representative experiment ($n = 2$) of 3 independent experiments. **, $P < 0.01$; ***, $P < 0.005$, *S*tudent *t* test. **C** and **D,** mRNA expression of AXIN2 and TCF7 was evaluated by real-time PCR in $CD4^+$ T cells at day 1, after $CD4^+CD45RA^+$ TN cell culture with conditioned media from NTUM and TUM liver tissue fragments (at different dilutions 1:10/1:100 in compete RPMI medium). The graphs showed 1representative experiment ($n = 2$) of 5 independent experiments. *, $P < 0.05$; **, $P < 0.01$, Student *t* test. **E,** Representative T-bet/Eomes expression by FC analysis within $CD4^+$ T-cell subset at 7 days. $CD4^+CD45RA^+$ TN cells were cultured with TWS119 (5 μmol/L), conditioned media (from NTUM and TUM liver tissue fragments) at different dilutions (1:10/1:100 in complete RPMI) compared with controls (NT and DMSO at the concentration of 5 μmol/L). **F,** The graph indicated the percentage of $Eomes^+$ and T-bet^+ cells in the $CD4^+$ T-cell subset, at day 7. $CD4^+CD45RA^+$ TN cells were treated with TWS119 (5 μmol/L) and conditioned media (from NTUM and TUM liver tissue fragments) at different dilutions (1:10/1:100 in complete RPMI) compared with controls (NT and DMSO at the concentration of 5 μmol/L). *, $P < 0.05$; ***, $P < 0.005$; ****, $P < 0.0001$, Student *t* test. **G,** The graph displayed the MFI of T-bet in gated $CD4^+$ T-cell subset after 7 days of $CD4^+CD45RA^+$ TN cell culture with conditioned media (from NTUM and TUM liver tissue fragments) diluted at the concentration of 1:10 in complete RPMI medium. The graph presented 1 representative experiment ($n = 2$) of 3 independent experiments. *, $P < 0.05$; **, $P < 0.01$, Student *t* test. **H,** The graph showed the MFI of T-bet, in the gated $CD4^+$ T-cell subpopulation, evaluated after 7 days of culture of $CD4^+CD45RA^+$ TN cells with DMSO (5 μmol/L), TWS119 (5 μmol/L), and conditioned media from NTUM liver fragments diluted at a concentration of 1:10 in complete RPMI medium in the experiment was added anti-Wnt3a at the concentration of 15 ng/mL. The concentration of Wnt3a in the conditioned media was evaluated (for the culture of $CD4^+CD45RA^+$ TN cells) by ELISA assay. The amount of Wnt3a was around 50–60 ng/mL. The graph showed 1 representative experiment ($n = 3$) out of 3 independent experiments. *, $P < 0.05$, Student *t* test.

may interfere with the inhibitory Wnt/β-catenin signals received by dendritic cells from the tumor microenvironment that, in turn, can improve the generation of functional Teff cells (15, 39–42).

In a companion study (43) submitted with this article, we provide evidence showing that Wnt3a blockade drives expansion of tumor antigen-specific $CD8^+$ Teff cells and a reduction of tumor mass through the help of dendritic cells *in vivo*. Our combined human and mouse studies may pave the way for exploiting Wnt3a antagonists in unleashing antitumor T-cell responses.

Disclosure of Potential Conflicts of Interest

No potential conflicts of interest were disclosed.

Authors' Contributions

Conception and design: V. Schinzari, E. Timperi, G.L. Grazi, V. Barnaba
Development of methodology: G. Pecora, V. Barnaba
Acquisition of data (provided animals, acquired and managed patients, provided facilities, etc.): V. Schinzari, E. Timperi, F. Palmucci, D. Gallerano, A. Grimaldi, D.A. Covino, N. Guglielmo, F. Melandro, E. Manzi, A. Sagnotta, F. Lancellotti, L. Sacco, P. Chirletti, G.L. Grazi, M. Rossi
Analysis and interpretation of data (e.g., statistical analysis, biostatistics, computational analysis): V. Schinzari, E. Timperi, F. Palmucci, D. Gallerano, A. Grimaldi, E. Manzi, V. Barnaba
Writing, review, and/or revision of the manuscript: V. Schinzari, E. Timperi, G.L. Grazi, V. Barnaba
Administrative, technical, or material support (i.e., reporting or organizing data, constructing databases): V. Schinzari, E. Timperi, D. Gallerano, E. Manzi, F. Lancellotti,
Study supervision: V. Schinzari, E. Timperi, G.L. Grazi, V. Barnaba

Acknowledgments

This work was supported by the following grants: Associazione Italiana per la Ricerca sul Cancro (AIRC; progetti "Investigator Grant" [IG]-2014 id. 15199 and IG-2017 id. 19939); Ministero della Salute (Ricerca finalizzata; RF-2010-2310438 and RF 2010-2318269); Fondazione Italiana Sclerosi Multipla (FISM) onlus (cod. 2015/R/04); Ministero dell'Istruzione, dell'Università e della Ricerca (MIUR; PRIN 2010-2011 prot. 2010LC747T_004); Fondo per gli investimenti di ricerca di base (FIRB)-2011/13 (no. RBAP10TPXK); Istituto Pasteur Italia – Fondazione Cenci Bolognetti (grant 2014-2016); and International Network Institut Pasteur, Paris—"Programmes Transversaux De Recherche" (PTR n. 20-16).

The authors thank Prof. Gabriella Girelli (Director UOC di Immunoematologia e Medicina Trasfusionale, "Sapienza" Università di Roma, Italy) for providing us buffy coats of blood donors. We extend special thanks to the patients who participated in this study.

The costs of publication of this article were defrayed in part by the payment of page charges. This article must therefore be hereby marked *advertisement* in accordance with 18 U.S.C. Section 1734 solely to indicate this fact.

Received December 7, 2017; revised March 26, 2018; accepted June 12, 2018; published first July 17, 2018.

References

1. van Amerongen R, Nusse R. Towards an integrated view of Wnt signaling in development. Development 2009;136:3205–14.
2. Clevers H, Nusse R. Wnt/β-catenin signaling and disease. Cell 2012;149:1192–205.
3. Gattinoni L, Ji Y, Restifo NP. Wnt/β-catenin signaling in T-cell immunity and cancer immunotherapy. Clin Cancer Res 2010;16:4695–701.
4. Clevers H. Wnt/β-catenin signaling in development and disease. Cell 2006;127:469–80.
5. Aberle H, Bauer A, Stappert J, Kispert A, Kemler R. β-catenin is a target for the ubiquitin-proteasome pathway. EMBO J 1997;16:3797–804.
6. Staal FJ, Luis TC, Tiemessen MM. WNT signaling in the immune system: WNT is spreading its wings. Nat Rev Immunol 2008;8:581–93.
7. Anastas JN, Moon RT. WNT signaling pathways as therapeutic targets in cancer. Nat Rev Cancer 2013;13:11–26.
8. Inagawa S, Itabashi M, Adachi S, Kawamoto T, Hori M, Shimazaki J, et al. Expression and prognostic roles of β-catenin in hepatocellular carcinoma: correlation with tumor progression and postoperative survival. Clin Cancer Res 2002;8:450–6.
9. Pan LH, Yao M, Cai Y, Gu JJ, Yang XL, Wang L, et al. Oncogenic Wnt3a expression as an estimable prognostic marker for hepatocellular carcinoma. World J Gastroenterol 2016;22:3829–36.
10. Voloshanenko O, Erdmann G, Dubash TD, Augustin I, Metzig M, Moffa G, et al. Wnt secretion is required to maintain high levels of Wnt activity in colon cancer cells. Nat Commun 2013;4:2610.
11. Augustin I, Dewi DL, Hundshammer J, Rempel E, Brunk F, Boutros M. Immune cell recruitment in teratomas is impaired by increased Wnt secretion. Stem Cell Res 2016;17:607–15.
12. Chien AJ, Moore EC, Lonsdorf AS, Kulikauskas RM, Rothberg BG, Berger AJ, et al. Activated Wnt/β-catenin signaling in melanoma is associated with decreased proliferation in patient tumors and a murine melanoma model. Proc Natl Acad Sci U S A 2009;106:1193–8.
13. Yaguchi T, Goto Y, Kido K, Mochimaru H, Sakurai T, Tsukamoto N, et al. Immune suppression and resistance mediated by constitutive activation of Wnt/β-catenin signaling in human melanoma cells. J Immunol 2012;189:2110–7.
14. Fu C, Liang X, Cui W, Ober-Blobaum JL, Vazzana J, Shrikant PA, et al. β-Catenin in dendritic cells exerts opposite functions in cross-priming and maintenance of CD8+ T cells through regulation of IL-10. Proc Natl Acad Sci U S A 2015;112:2823–8.
15. Spranger S, Bao R, Gajewski TF. Melanoma-intrinsic β-catenin signaling prevents anti-tumour immunity. Nature 2015;523:231–5.
16. Spranger S, Gajewski TF. A new paradigm for tumor immune escape: β-catenin-driven immune exclusion. J Immunother Cancer 2015;3:43.
17. Spranger S, Gajewski TF. Tumor-intrinsic oncogene pathways mediating immune avoidance. Oncoimmunology 2016;5:e1086862.
18. Driessens G, Zheng Y, Locke F, Cannon JL, Gounari F, Gajewski TF. β-catenin inhibits T cell activation by selective interference with linker for activation of T cells-phospholipase C-gamma1 phosphorylation. J Immunol 2011;186:784–90.
19. Zhao DM, Yu S, Zhou X, Haring JS, Held W, Badovinac VP, et al. Constitutive activation of Wnt signaling favors generation of memory CD8 T cells. J Immunol 2010;184:1191–9.
20. Zhou X, Yu S, Zhao DM, Harty JT, Badovinac VP, Xue HH. Differentiation and persistence of memory CD8(+) T cells depend on T cell factor 1. Immunity 2010;33:229–40.
21. Kim EH, Sullivan JA, Plisch EH, Tejera MM, Jatzek A, Choi KY, et al. Signal integration by Akt regulates CD8 T cell effector and memory differentiation. J Immunol 2012;188:4305–14.
22. Gattinoni L, Lugli E, Ji Y, Pos Z, Paulos CM, Quigley MF, et al. A human memory T cell subset with stem cell-like properties. Nat Med 2011;17:1290–7.
23. Gattinoni L, Zhong XS, Palmer DC, Ji Y, Hinrichs CS, Yu Z, et al. Wnt signaling arrests effector T cell differentiation and generates CD8+ memory stem cells. Nat Med 2009;15:808–13.
24. Heikamp EB, Patel CH, Collins S, Waickman A, Oh MH, Sun IH, et al. The AGC kinase SGK1 regulates TH1 and TH2 differentiation downstream of the mTORC2 complex. Nat Immunol 2014;15:457–64.
25. Schreiber RD, Old LJ, Smyth MJ. Cancer immunoediting: integrating immunity's roles in cancer suppression and promotion. Science 2011;331:1565–70.
26. Timperi E, Focaccetti C, Gallerano D, Panetta M, Spada S, Gallo E, et al. IL-18 receptor marks functional CD8+ T cells in non-small cell lung cancer. Oncoimmunology 2017;6:e1328337.
27. Timperi E, Pacella I, Schinzari V, Focaccetti C, Sacco L, Farelli F, et al. Regulatory T cells with multiple suppressive and potentially pro-tumor activities accumulate in human colorectal cancer. Oncoimmunology 2016;5:e1175800.
28. Wherry EJ, Kurachi M. Molecular and cellular insights into T cell exhaustion. Nat Rev Immunol 2015;15:486–99.
29. Rubio V, Stuge TB, Singh N, Betts MR, Weber JS, Roederer M, et al. Ex vivo identification, isolation and analysis of tumor-cytolytic T cells. Nat Med 2003;9:1377–82.
30. Edge SB, Compton CC. The American Joint Committee on Cancer: the 7th edition of the AJCC cancer staging manual and the future of TNM. Ann Surg Oncol 2010;17:1471–4.
31. Schumacher TN, Schreiber RD. Neoantigens in cancer immunotherapy. Science 2015;348:69–74.
32. Snyder A, Makarov V, Merghoub T, Yuan J, Zaretsky JM, Desrichard A, et al. Genetic basis for clinical response to CTLA-4 blockade in melanoma. N Engl J Med 2014;371:2189–99.

Published OnlineFirst July 17, 2018; DOI: 10.1158/2326-6066.CIR-17-0712

33. Watson IR, Takahashi K, Futreal PA, Chin L. Emerging patterns of somatic mutations in cancer. Nat Rev Genet 2013;14:703–18.
34. Sharma P, Allison JP. The future of immune checkpoint therapy. Science 2015;348:56–61.
35. Hellmann MD, Rizvi NA, Goldman JW, Gettinger SN, Borghaei H, Brahmer JR, et al. Nivolumab plus ipilimumab as first-line treatment for advanced non-small-cell lung cancer (CheckMate 012): results of an open-label, phase 1, multicohort study. Lancet Oncol 2017;18:31–41.
36. Postow MA, Chesney J, Pavlick AC, Robert C, Grossmann K, McDermott D, et al. Nivolumab and ipilimumab versus ipilimumab in untreated melanoma. N Engl J Med 2015;372:2006–17.
37. Utzschneider DT, Charmoy M, Chennupati V, Pousse L, Ferreira DP, Calderon-Copete S, et al. T cell factor 1-expressing memory-like CD8 (+) T cells sustain the immune response to chronic viral infections. Immunity 2016;45:415–27.
38. Jeannet G, Boudousquie C, Gardiol N, Kang J, Huelsken J, Held W. Essential role of the Wnt pathway effector Tcf-1 for the establishment of functional CD8 T cell memory. Proc Natl Acad Sci U S A 2010;107:9777–82.
39. Jiang A, Bloom O, Ono S, Cui W, Unternaehrer J, Jiang S, et al. Disruption of E-cadherin-mediated adhesion induces a functionally distinct pathway of dendritic cell maturation. Immunity 2007;27:610–24.
40. Manicassamy S, Reizis B, Ravindran R, Nakaya H, Salazar-Gonzalez RM, Wang YC, et al. Activation of β-catenin in dendritic cells regulates immunity versus tolerance in the intestine. Science 2010;329:849–53.
41. Oderup C, LaJevic M, Butcher EC. Canonical and noncanonical Wnt proteins program dendritic cell responses for tolerance. J Immunol 2013;190:6126–34.
42. Suryawanshi A, Manicassamy S. Tumors induce immune tolerance through activation of β-catenin/TCF4 signaling in dendritic cells: A novel therapeutic target for cancer immunotherapy. Oncoimmunology 2015;4:e1052932.
43. Pacella I, Cammarata I, Focaccetti C, Miacci S, Gulino A, Tripodo C, et al. Wnt3a neutralization indirectly favors anti-tumor T cell response and restrains tumor growth in a mouse cancer model. Cancer Immunol Res 2018 July 17. [Epub ahead of print].

AACR American Association for Cancer Research

Cancer Immunology Research

Wnt3a/β-Catenin Signaling Conditions Differentiation of Partially Exhausted T-effector Cells in Human Cancers

Valeria Schinzari, Eleonora Timperi, Giulia Pecora, et al.

Cancer Immunol Res 2018;6:941-952. Published OnlineFirst July 17, 2018.